İSTANBUL UNIVERSITY CERRAHPAŞA

ORIGINAL ARTICLE
Electrica 2022; 22(2): 198-210

Improved Performance of Doubly-Fed Induction Generator Wind Turbine During Transient State Considering Supercapacitor Control Strategy

Kenneth E. Okedu[1,2]

[1]Department of Electrical and Communication Engineering, National University of Science and Technology, Muscat, Sultanate of Oman
[2]Department of Electrical and Electronic Engineering, Nişantaşı University, Istanbul, Turkey

Cite this article as: K. E. Okedu, "Improved performance of doubly-fed induction generator wind turbine during transient state considering supercapacitor control strategy," *Electrica.*, 22(2), 198-210, 2022.

ABSTRACT

This paper proposes a supercapacitor strategy for improving the capability of grid-connected doubly-fed induction generator (DFIG) wind turbines during fault scenarios. Supercapacitors are one of the important components in sustainable energy systems that are commonly used to store energy. In DFIGs, the supercapacitor is used to compensate for voltage dips and damping oscillations. In this work, a new topology of the supercapacitor system was used to investigate a DFIG wind turbine during transient state. The model system employed was a DFIG connected to the earlier wind turbine technology of fixed speed squirrel cage induction generator. Efforts were made to determine the effective parameters and switching strategies of the supercapacitor by considering different scenarios, in order to improve the transient state of the wind generator. The results obtained under severe grid fault were compared considering the different parameters of the resistance, inductance, and capacitance of the supercapacitor. The DC-link voltage and grid voltage switching strategies of the supercapacitor were investigated. Furthermore, the results of the proposed DFIG supercapacitor were compared with the traditional parallel capacitor scheme for DFIG system. For a fair comparison between the DFIG supercapacitor and parallel capacitor-based solution, the capacitance value considered was the same to buffer the transient energy.

Index Terms—DFIG, supercapacitor, transients, wind energy, wind turbine

I. INTRODUCTION

Recently, the use of renewable energy technology has been gaining attention. Among the renewable energy sources, wind energy is widely used because of the high-energy transfer capability technology in wind turbine applications. Variable-speed wind turbines are the main contributors to wind power generation. In order to help achieve energy transfer capability at peak level, the doubly-fed induction generators (DFIGs) are widely employed in the development of recent wind farms and wind power generation systems [1,2]. The control of wind farms and their impacts on the security and stability of power grids have become key areas of focus in wind energy applications, due to the continuous increase of installed wind power capacity, control schemes [3], stability improvement [4], dynamic regulation mechanisms [5], and approach [6]. However, grid-connected DFIG-based wind turbines are very sensitive to certain transient stability situations, and many studies in the literature have developed various schemes to eliminate them. The DC component of the generated current on the stator of the wind turbine cuts the rotor windings, when the grid voltage decreases abruptly, resulting in excessive rotor current and DC bus overvoltage. Consequently, the wind turbine should be disconnected from the grid, and several power electronic devices in the wind power generation system could be damaged. Therefore, wind power grid connection guidelines require most grid operators to handle low-voltage ride-through (LVRT) or fault-ride-through (FRT) during the occurrence of grid voltage sags.

The DFIG wind turbine usually consists of a rotor side converter (RSC) that achieves maximum power point tracking (MPPT) and a grid side converter (GSC) that regulates the DC-link [7,8]. This type of wind turbine is widely popular because only a partially rated wind energy conversion system that is about 25–30% of the system rating is necessary [9], leading to a higher efficiency and lower converter cost [10]. However, because the GSC is directly tied to the power grid in

Corresponding author:
Kenneth E. Okedu

E-mail: okedukenneth@nu.edu.om or kenokedu@yahoo.com

Received: January 12, 2022

Revised: February 3, 2022

Accepted: March 3, 2022.

DOI: 10.54614/electrica.2022.21006

the DFIG system, severe rotor and stator transients may occur during grid disturbances, making the wind energy conversion system vulnerable [11,12].

There are concerns regarding the stability and the reliability of the power grid [13,14], as a result of the increasing penetration of wind energy systems. Therefore, a stricter grid code is required to be applied to wind energy systems to protect the existing grid standards [15]. Low-voltage ride-through is a grid code requirement that is implemented in many countries, which requires wind turbines to be grid connected during voltage dips for grid voltage support and fast system recovery [16]. However, during a voltage dip, the power that can be transferred to the grid is greatly limited causing a power imbalance between the RSC and the GSC, which charges the DC-link. Furthermore, for DFIGs, voltage dips will also cause severe rotor and stator current transients because the stator is directly connected to the grid [17-19]. Therefore, LVRT enhancement methods are required for DFIGs. References [10] and [14] have provided a comprehensive overview of existing DFIG LVRT strategies. To handle LVRT of DFIGs in wind farms, various methods for the RSC have been devised to improve both the hardware utilization rate and LVRT handling. The existing methods mainly include proportional current tracking control [20], flux tracking control [21], transient current feedforward control [22], active damping control [23], and robust control [24,25]. In [20], a scaled current tracking control for RSC was used to enhance the LVRT capacity of DFIG without flux observation. In this scheme, the rotor current was controlled to track stator current in a certain scale, considering proper tracking coefficient, within permissible ranges to maintain the DFIG overcurrent and overvoltage. Uses a negative sequence current compensation scheme to smooth the electromagnetic torque and reactive power for asymmetrical grid faults and traditional vector Control for reactive power to suppress the grid voltage during symmetrical grid faults [21]. A feedforward current references control scheme for the RSC of the DFIG was used in [22], to improve the transient of the wind generator. An additional feedforward rotor current reference was introduced in the current loop to enhance the tracking ability and control targets. Although the above control strategy can improve the LVRT capability of DFIG to a certain extent, it is incapable of adapting to the varying grid conditions. This may result in the problem of control lag and a large control deviation while handling LVRT.

The energy storage systems (ESS) model is one of the most widely used control strategies in wind energy conversion systems. One of the ESS elements is a supercapacitor that enables smooth output power, with the ability to mitigate oscillations. Constant power control could be provided in DFIG wind turbines by using the supercapacitor model. In the literature, a management control unit has been developed to provide power tracking in a two-layer control scheme in Reference [26] and constant power control in [27,28], considering the supercapacitor model. In [29], a study on the suppression of power fluctuation in DFIG based on supercapacitor energy storage was carried out, in order to improve its performance. The study elaborated that supercapacitors could be used in DFIGs to obtain constant output power as well as to prevent frequency changes of switching elements in the converter circuit. The study monitored the maximum power point of a DFIG wind turbine, considering the supercapacitors scheme. In another study carried out in References [30,31], the responses to the change in wind speed, tower shadow, and the protection units were investigated. The supercapacitor model was selected in order to optimize energy production and consumption by adjusting the output power in the DFIG. The safe and effective use of the supercapacitors was observed under optimal operating conditions in References [32,33], for a battery hybrid energy storage system and wind energy integration. In addition to ensuring optimum operating conditions, a coordinated control was carried out in the DFIG wind turbine considering the supercapacitor scheme in two stages for optimal active power control management [34].

The supercapacitor was selected in order to provide pitch angle control in the DFIG because of its advantages that include high performance, high-temperature operating ability, long service life, and convenient use in applications [35]. A hybrid model design was realized using the power electronics drives of a supercapacitor and a double-layer capacitor, and the response times in the transient state were improved in [36,37]. The effects of the supercapacitor on small signal stability were analyzed based on frequency stability, and the effects of the supercapacitor on the frequency ratio, operating mode, and participation factor were interpreted in [38]. Transient analysis of the supercapacitor for active and reactive power control in a DFIG has been examined in the literature. Moreover, short-circuit effects were minimized by providing flux and voltage control in the back-to-back converter circuit [15]. Depending on the maximum and minimum frequency values, the inertial model and the supercapacitor were used together in a DFIG for system reliability, and comparisons of conditions with and without supercapacitors were investigated in [40-43]. Various supercapacitor control models have been developed for DFIG LVRT capability in the literature [44,45], thus, the adverse situations that may occur in grid-connected DFIGs can be eliminated. However, these models, which have been developed in some robust DFIG applications, may be insufficient due to inrush currents and over-voltages.

In this paper, a new control strategy of a supercapacitor system is examined for a DFIG wind turbine during severe grid fault condition. A simple two-machine model system consisting of a DFIG connected to a fixed-speed squirrel cage induction generator wind turbine was used in carrying out the transient analysis in this study. The supercapacitor system was connected across the terminals of the DC-link voltage of the DFIG wind turbine, between the RSC and the GSC. The study considered the determination of the effective parameters of the supercapacitor in the DFIG wind turbine, by considering different values of resistance, inductance, and capacitance of the supercapacitor, in various scenarios. Furthermore, two switching strategies of the embedded supercapacitor system in the DFIG, the DC-link voltage and the grid voltage, were investigated using the various values earlier considered. The obtained results were compared with those using parallel capacitor scheme for the DFIG connected to the RSC and GSC of the wind turbine. For effective comparative study, between the supercapacitor and parallel capacitor-based solution to buffer the transient energy of the DFIG, the same capacitance value was employed in the study. The proposed supercapacitor scheme for the DFIG wind turbine has the ability to store a large amount of electric charge compared to the parallel capacitors and all other types of conventional capacitors. This is because the charge storage, which is the capacitance in conventional capacitors, is directly proportional to the surface area of each electrode or plate and inversely proportional to the distance between them. The topology of capacitors and batteries in wind turbines differs in two ways considering the amount of charge or energy storage and how quickly the charge or energy is dissipated. The batteries have the ability to store more energy than the conventional capacitors; however, the shortcoming of the batteries is they cannot deliver the stored energy very quickly. Though the capacitors deliver the stored energy more quickly, however, they lack the ability to store large amount of energy as the batteries. These two shortcomings could be overcome by using the proposed supercapacitors in DFIG wind turbines. This is because the supercapacitors have large surface area electrodes and very thin dielectric, as separating distance between the electrodes. Thus, compared to the conventional capacitors, the supercapacitors have very small distance between the electrodes, making it possible to obtain larger capacitance or energy storage that is delivered quickly to help improve the performance of the DFIG wind turbine variables during transient state.

II. MODELING AND CONTROL

A. Wind Turbine Characteristics

The DFIG wind turbine torque and mechanical extracted power are given as follows in (1) and (2), respectively [46,47].

$$T_m = \frac{\pi \rho R^3}{2} V_w^2 C_t(\lambda)[\mathrm{Nm}] \tag{1}$$

$$P_m = \frac{\pi \rho R^2}{2} V_w^3 C_p(\lambda)[\mathrm{W}] \tag{2}$$

where ρ is the air density, R is the radius of the turbine, V_w is the wind speed, and $C_p(\lambda, \beta)$ is the power coefficient given by

$$C_p(\lambda,\beta)=0.5(\Gamma-0.02\beta^2-5.6)e^{-0.17\Gamma} \tag{3}$$

C_t and C_p are related by

$$C_t(\lambda)=\frac{C_p(\lambda)}{\lambda} \tag{4}$$

$$\lambda=\frac{\omega_r R}{V_w} \tag{5}$$

$\Gamma=\frac{R}{\lambda}\frac{(3600)}{(1609)}$ from (3), and ratio of the speed tip is λ.

The DFIG wind turbine characteristics are shown in Fig. 1. The DFIG rotor speed range is between 0.7 p.u. to 1.3 p.u. and the maximum power is obtained when the turbine speed is at 0.97 p.u.

B. Doubly-Fed Induction Generator *Model and Control*

Details of the DFIG model and control can be obtained from [48-51]. The RSC control of the DFIG in Fig. 2 is regulated by the axes q and d currents i_{qr} and i_{dr}. This is done by (P_s, Q_s), of the stator. The MPPT obtains the P_s. In Fig. 3, the GSC of the wind generator employs the power grid alternating current reference frame to control the voltage of the DC-link and exchange of reactive power at the point of common coupling, based on the direction of power flow in the rotor circuitry. The *dq*/*abc* transformation and vice versa regarding the grid voltage for synchronism are obtained via the in-built phase-locked loop model.

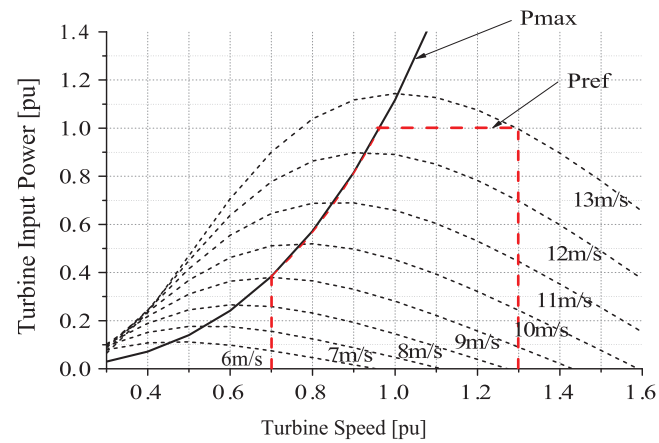

Fig. 1. The wind turbine characteristics.

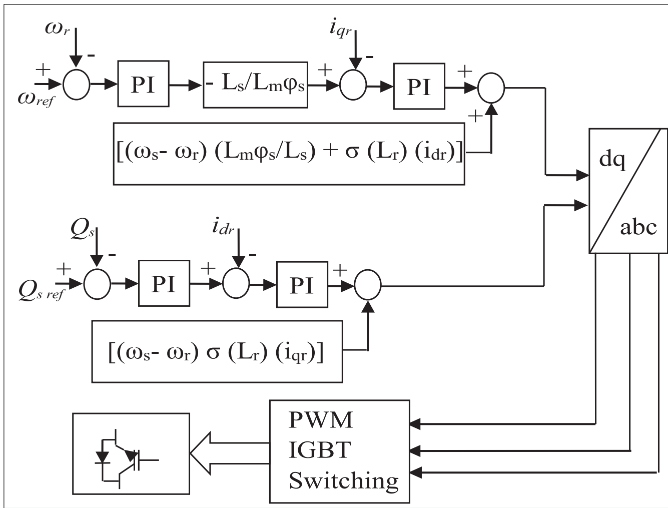

Fig. 2. The rotor side converter control circuit of the doubly-fed induction generator.

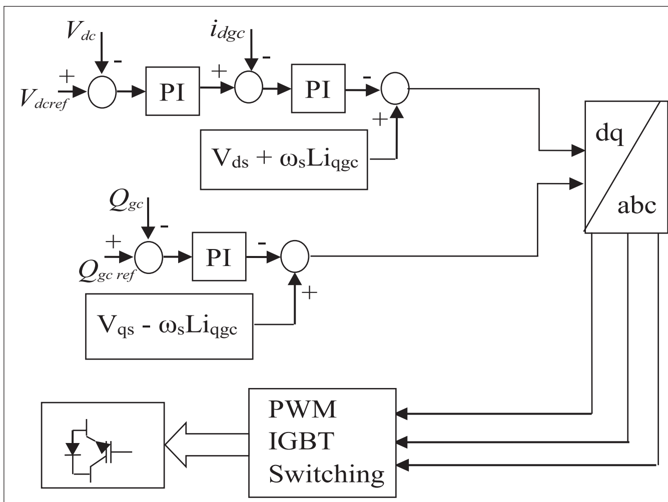

Fig. 3. The grid side converter control circuit of the doubly-fed induction generator.

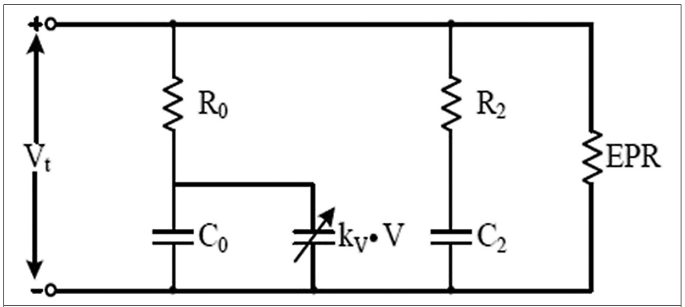

Fig. 4. Traditional supercapacitor model.

III. THE DOUBLY-FED INDUCTION GENERATOR MODEL WITH SUPERCAPACITOR SYSTEM

A. The Dynamics of the Traditional Supercapacitor System

The traditional simple electrical equivalent model of the supercapacitor is shown in Fig. 4. The model cell capacity expression is given by [52-54]:

$$C_{cell}=C_0+K_v V_c \tag{6}$$

The total capacity expressions for *n* numbers in the series for the model system are:

$$C_{total}=\frac{1}{\frac{1}{C_{cell1}}+\frac{1}{C_{cell2}}+\frac{1}{C_{cell3}}+\& \frac{1}{C_{celln}}} \tag{7}$$

$$C_{total}=\frac{1}{n}C_{cell}=\frac{1}{n}(K_v V_c) \tag{8}$$

The model terminal voltage equations and the capacity chance over time are expressed as:

$$V(t)=\mathrm{i}(t)R+\frac{1}{C_{total}}\int \mathrm{i}(t)\mathrm{d}t \tag{9}$$

$$V(t)=V_C(t)+(C_0+K_v V_c)(R_0+R_2)+\frac{\mathrm{d}V_c(t)}{\mathrm{d}t} \tag{10}$$

$$\frac{\mathrm{d}V_c}{\mathrm{d}t}=\frac{V-V_c}{(R_0+R_2)(C_0+K_v V_c)} \tag{11}$$

In the supercapacitor model in Fig. 4, depending on the number of cells, the use of multiple resistors can be represented by equivalent series resistance and equivalent parallel resistance. The voltage and initial voltage equations using the equivalent series resistors are given by:

$$V(t)=R_{ESR}i(t)+\frac{1}{C_{total}}\int i(t)\mathrm{d}t \tag{12}$$

$$V_0=R_{ESR}i(t)+\frac{1}{C_{total}}\int i(t)\mathrm{d}t \tag{13}$$

$$R_{ESR}+C_{total}\frac{\mathrm{di}(t)}{\mathrm{d}t}-i(t)=0 \tag{14}$$

The charge and discharge expressions in the supercapacitor system are given in (15) and (16), respectively, while the expression for the terminal voltage as a function of time is given in (17).

$$V_r(t)=Ke^{\frac{1}{R_{ESR}+C_{total}}t} \tag{15}$$

$$\frac{\mathrm{d}V_c}{\mathrm{d}t}=\frac{-V_c}{(R_o+R_2)(C_0+K_v V_c)} \tag{16}$$

$$V_t(t)=V_c(t)+V_r(t) \tag{17}$$

B. *The Dynamics of the Supercapacitor System in* Doubly-Fed Induction Generator *Wind Turbines*

The connection of the supercapacitor in the DFIG is shown in Fig. 5, where P is the grid side transformer power, P_{grid} is the power of the grid, P_s is the stator power, P_r is the rotor power, and $P_{supercapacitor}$ is the power of the supercapacitor. In the DFIG, the supercapacitor is able to adjust the DC bus voltage value in the range of 0–100%. While a certain part of the power values are met by the grid in the creation of the supercapacitor model, the remaining power values are met by the DFIG. The amount of energy and capacity expressions stored in the supercapacitor are given in (18)–(20).

$$E_{supercapacitor}=0.2P_{nominal}t \tag{18}$$

$$E_{supercapacitor}=\frac{1}{2}C_{supercapacitor}\left(V_{max}^2-V_{min}^2\right) \tag{19}$$

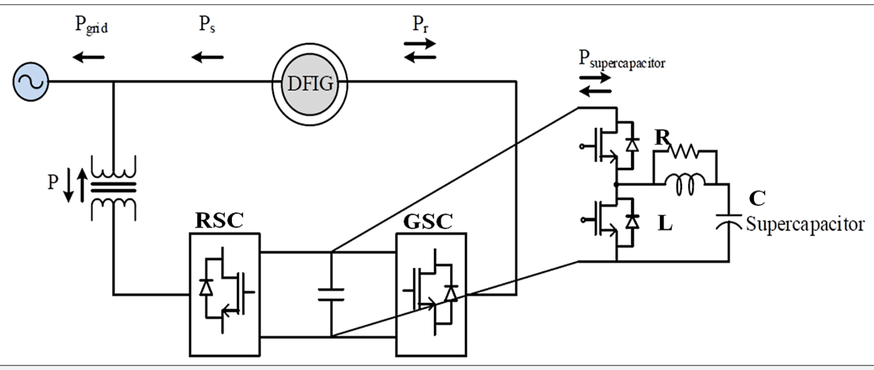

Fig. 5. Doubly-fed induction generator with the proposed supercapacitor topology.

$$C_{supercapacitor} = \frac{0.4P_{nominal}t}{V_{max}^2 - V_{min}^2} \quad (20)$$

where $E_{supercapacitor}$ is the amount of energy in the supercapacitor, $P_{nominal}$ is the nominal power value, t is the supercapacitor operating time, $C_{supercapacitor}$ is the supercapacitor capacity value, V_{max} is the maximum supercapacitor voltage, and V_{min} is the minimum supercapacitor voltage, respectively.

IV. THE MODEL SYSTEM OF STUDY AND PARAMETERS

The model system used for this study is shown in Fig. 6(a), and the related parameters of the wind turbines are given in Table I. The excitation parameters of the DFIG are given in Table II, while the parameters of the supercapacitor system for the different cases considered are given in Table III. In the model system of Fig. 6(a), the DFIG and IG wind turbines were connected to an infinite bus bar and subjected to a severe three phase to ground fault. The supercapacitor was connected to the terminals of the DFIG wind turbine in Fig. 6(a), as shown in Fig. 5.

The switching strategy of the supercapacitor is based on the DC-link voltage exceeding the set threshold of 110% of its nominal value during transient state or the grid voltage dropping below 1.0 p.u., as shown in Tables II and III, respectively. The parameter estimation procedure for the supercapacitor is described as follows based on Fig. 6(b). Generally, the models of the parameters usually have differential equations, transfer function, or block diagrams, that are updated offline or online. To obtain offline mode parameters, the process involves storing the data to use them much later, while for the online mode, it is based on parallel experiment [55]. However, there exist many procedures to achieve supercapacitor parameters like unscented Kalman filter [56] or the Luenberger-style scheme [57]. In this paper, the supercapacitor parameters were selected based on interactive, simple, and offline procedures [58] in Fig. 6(b) considering the Simscape model of Fig. 6(c), respectively.

TABLE I. PARAMETERS OF THE WIND TURBINES

Generator Type	IG	DFIG
Rated voltage	690 V	690 V
Stator resistance	0.01 p.u.	0.01 p.u.
Stator leakage reactance	0.07 p.u.	0.15 p.u.
Magnetizing reactance	4.1 p.u.	3.5 p.u.
Rotor resistance	0.007 p.u.	0.01 p.u.
Rotor leakage reactance	0.07 p.u.	0.15 p.u.
Inertia constant	1.5 seconds	1.5 seconds

IG, induction generator; DFIG, doubly-fed induction generator.

TABLE II. EXCITATION PARAMETERS AND SWITCHING THRESHOLD OF THE DOUBLY-FED INDUCTION GENERATOR WIND TURBINE

DC-Link Voltage	1.5 kV
DC-link capacitor	50,000 µF
Device for power converter	IGBT
PWM carrier frequency	2 kHz
Upper limit of DC voltage switching (E_{dc_Max})	1.65 kV (110%)
Lower limit of DC voltage switching (E_{dc_Min})	0.75 kV (50%)
Short circuit parameter of protective device for over-voltage	0.2 ohm
Grid voltage	≥1.0 *pu Normal condition* <1.0 *pu Faulty condition*

PWM: Pulse Width Modulation.

TABLE III. PARAMETERS AND SWITCHING STRATEGIES OF THE SUPERCAPACITOR

	DC-Link Voltage Switching Strategy			Grid Voltage Switching Strategy		
Case	R (Ω)	L (H)	C (F)	R (Ω)	L (H)	C (F)
1	0.1	1	1	0.1	1	1
2	0.2	2	2	0.2	2	2
3	0.3	3	3	0.3	3	3
4	0.1	1	1	0.1	1	1
5	0.2	2	2	0.2	2	2
6	0.3	3	3	0.3	3	3

V. SIMULATION RESULTS AND DISCUSSION

A. Evaluation of the Proposed Doubly-Fed Induction Generator Supercapacitor Scheme

Rigorous simulation studies were conducted to compare the fault ride through features of the DFIG supercapacitor-based system connected to a fixed-speed induction generator wind turbine shown in Fig. 6 model system. The system performance was evaluated using PSCAD/EMTDC [59] environment. The fault type is a severe symmetrical three-phase of 100 ms happening at 0.1 s, with the circuit breakers operation sequence opening and reclosing at 0.2 s and 1.0 s, respectively, on the faulted line at the fault point shown in the model system of Fig. 6(a). The fault performance with different parameters and switching strategies of the stability augmentation tool of the supercapacitor are presented below in detail.

The DFIG wind turbine with supercapacitor scheme was subjected to cases 1–6 in Table III, considering the excitation parameters and switching thresholds in Table II. Some of the simulation results for the cases considered are shown in Figs. 7-13. In Figs. 7 and 8, the DC-link voltage was not able to recover on time after the grid fault using both switching strategies of DC-link and grid voltage for cases 1, 4, 2, and 5, respectively. However, for cases 3 and 6, in Fig. 9, the performance of the DC-link voltage was the same for both switching strategies. Thus, the effective parameters of the supercapacitor for better performance of the DFIG wind turbine during the transient state are 0.3 Ω, 3*H*, 3*F*, for R, L, C, respectively, in Table III. Figs. 10–12 show the terminal voltage for the DFIG and IG wind turbines. From the figures, the parameters of the supercapacitors do not have effects on the responses of the terminal voltage of the wind turbines.

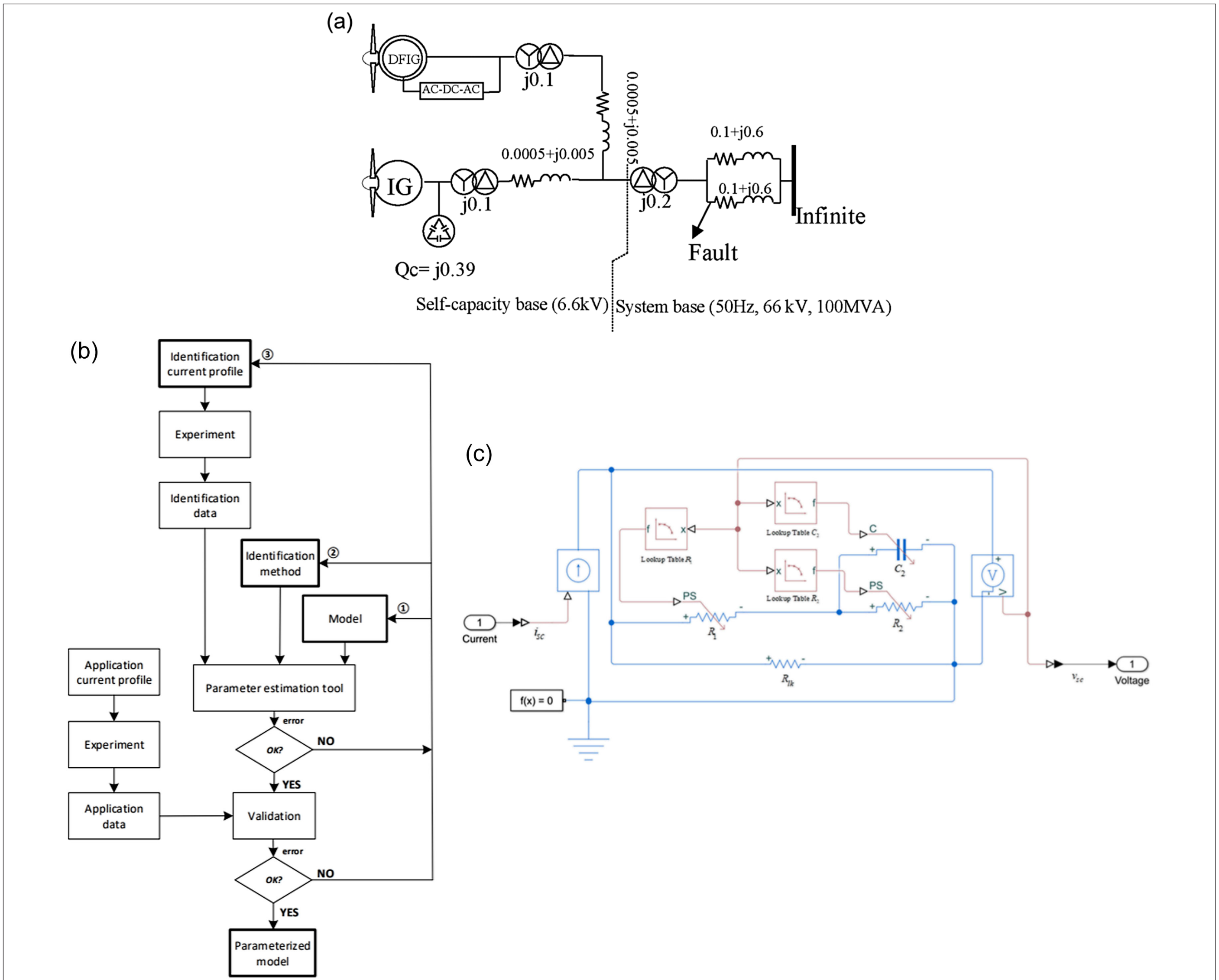

Fig. 6. (a) Model system of study. (b) Parameter estimation procedure. (c) Simscape model.

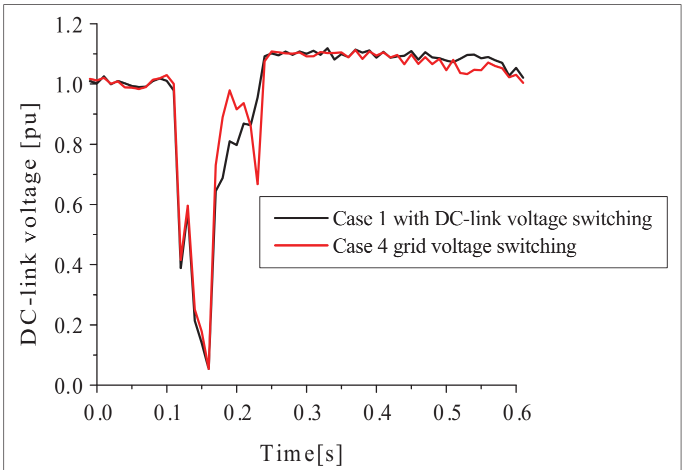

Fig. 7. DC-link voltage of doubly fed induction generator wind turbine (cases 1 and 4).

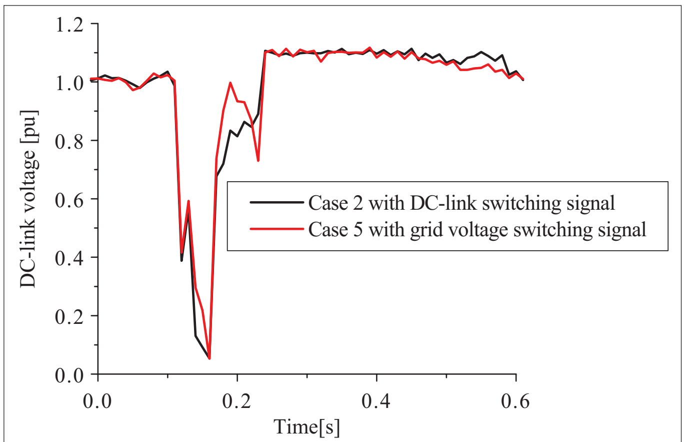

Fig. 8. DC-link voltage of doubly fed induction generator wind turbine (cases 2 and 5).

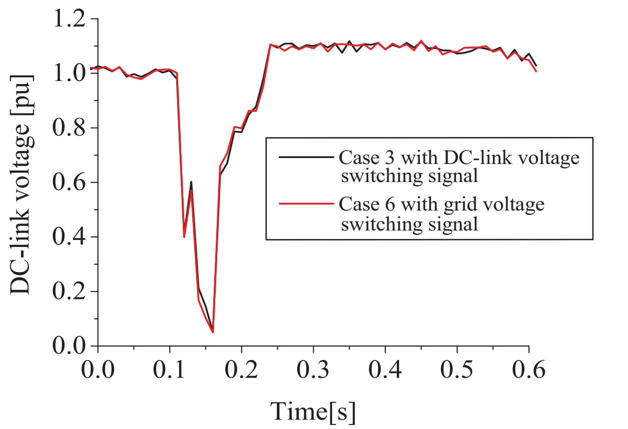

Fig. 9. DC-link voltage of doubly fed induction generator wind turbine (cases 3 and 6).

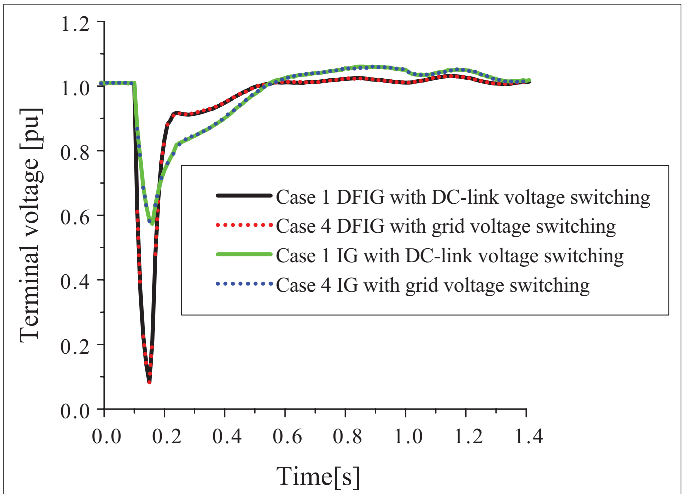

Fig. 10. Terminal voltage of DFIG and IG (cases 1 and 4).

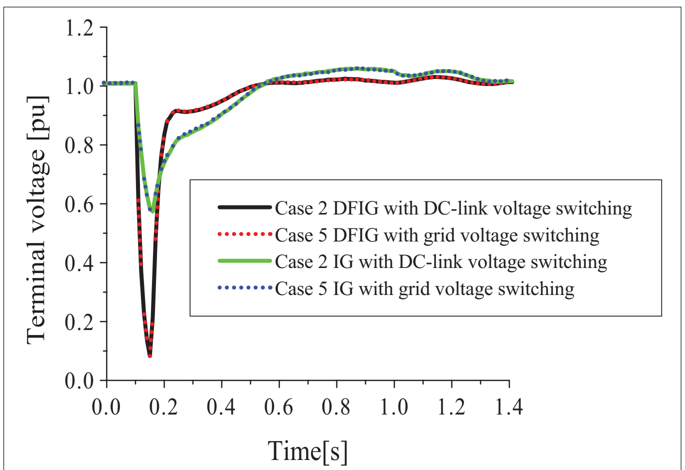

Fig. 11. Terminal voltage of DFIG and IG (cases 2 and 5).

In Fig. 13 (a and b), the active power was more influenced in case 6, compared to the other cases using the supercapacitor scheme, while in Fig. 14 (a and b), the reactive power was also more

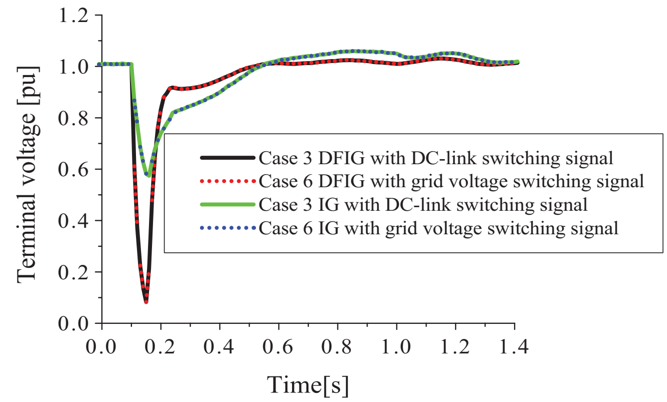

Fig. 12. Terminal voltage of DFIG and IG (cases 3 and 6).

dissipated or enhanced in case 6 compared to the other cases. It was also observed from the DFIG rotor speed performance in Fig. 15 (a) and (b) that the transient state performance in case 6 gave better response. Therefore, the effective parameters for the improved performance of the DFIG supercapacitor embedded system are when the resistance, inductance, and capacitance values are not too small. This is because the terminal voltage of the generator increases, mitigating the depression of the electrical torque and power. The supercapacitor will increase the mechanical power extracted from the drive train, thus reducing its speed excursion. Also, since mechanical torque is proportional to the square of the stator voltage of the DFIG, the effect would enhance the post fault recovery of the DFIG wind turbine.

B. Evaluation of the Proposed DFIG Supercapacitor Scheme and Parallel DFIG Capacitor Scheme

In this section, the proposed supercapacitor scheme and parallel capacitor-based scheme with the same capacitance value was evaluated for the DFIG, considering Fig. 16(a), with a conventional DC chopper circuit connected between the power converters of the wind turbine. The parallel capacitor scheme was connected at both the RSC and the GSC, and the switching strategy for both connections is shown in Fig. 16(b). Figure 16 shows the topology of the DFIG-based parallel capacitor scheme. The mathematical dynamics of connecting the parallel capacitor to the DFIG are given as follows.

As shown in Fig. 16, the power flowing via the DC-link circuit can be expressed as [48]:

$$P_{converter}=V_{dc}i_{dcr}=-V_{dc}i_{dcg}=-\frac{3}{2}v_{gq}i_{gq} \tag{21}$$

$$\left(C+C_p\right)\frac{dV_{dc}}{dt}=i_{dcg}+i_{dcr} \tag{22}$$

Putting the i_{dcg} term in (22) with i_{gq}, the DC-link voltage and q-component current relationship can be found as follows:

$$\left(C+C_p\right)\frac{dV_{dc}}{dt}=\frac{3}{2}\frac{v_{gq}i_{gq}}{V_{dc}}+i_{dcr} \tag{23}$$

In (23), the grid quantities are related to the first term, while the RSC injecting currents are associated with the second term. This rotor injecting current is an input disturbance caused by the power change. As a result, (23) can be re-written as

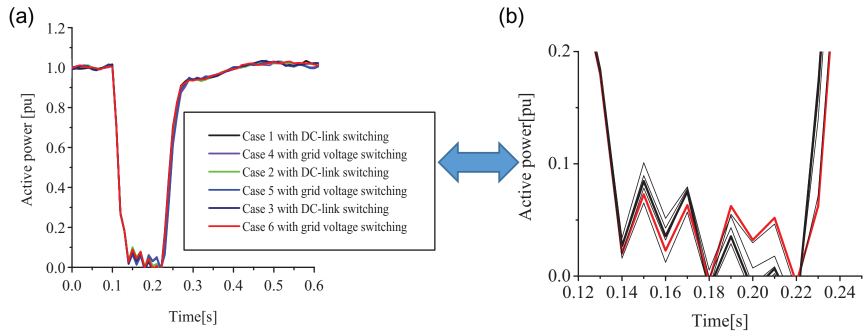

Fig. 13. (a) Active power of doubly-fed induction generator for all cases. (b) Zoom of (a).

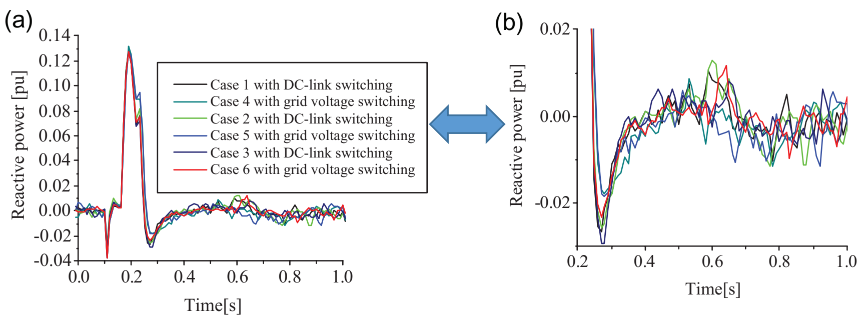

Fig. 14 (a). Reactive power of doubly-fed induction generator for all cases. (b) Zoom of (a).

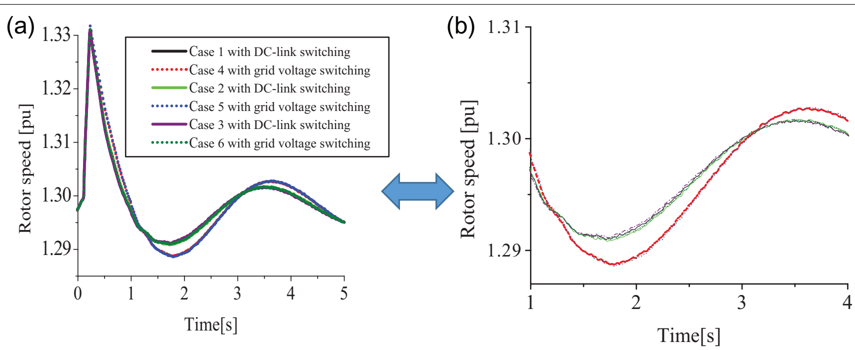

Fig. 15. (a) Rotor speed of doubly-fed induction generator for all cases. (b) Zoom of (a).

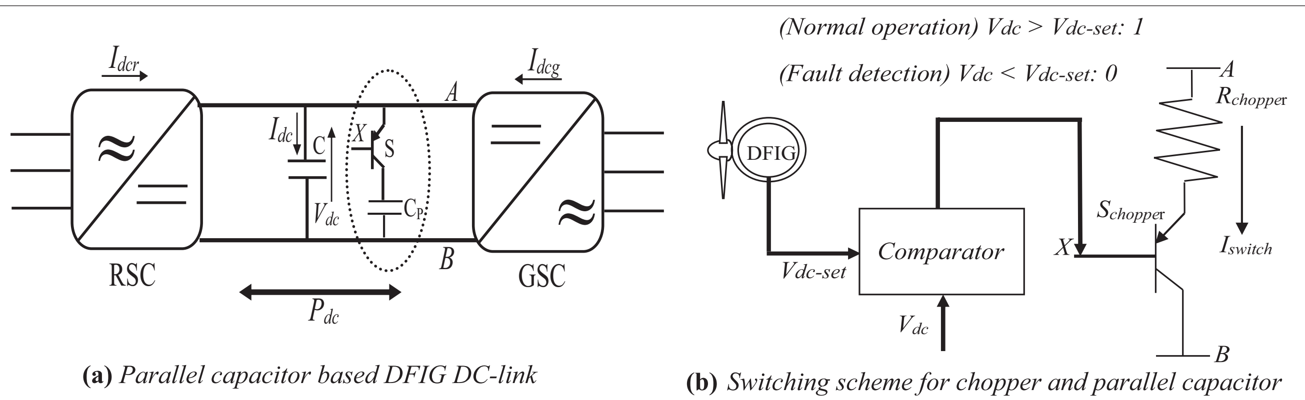

Fig. 16. Parallel capacitor topology for doubly-fed induction generator (DFIG) wind turbine. (a) Parallel capacitor-based DFIG DC-link. (b) Switching scheme for chopper and parallel capacitor.

$$\left(C+C_p\right)\frac{dV_{dc}}{dt}=\frac{3}{2}\frac{v_{gq}i_{gq}}{V_{dc}}+\frac{P_{converter}}{V_{dc}}=f \tag{24}$$

If (21) is differentiated with respect to all variables considering a given point $v_{gq0}, i_{gq0}, V_{dc0},$ then:

$$\left(C+C_p\right)\Delta V_{dc}=\frac{\partial f}{\partial i_{gq}}\Delta i_{gq}+\frac{\partial f}{\partial v_{gq}}\Delta v_{gq}+\frac{\partial f}{\partial V_{dc}}\Delta V_{dc}+\frac{\partial f}{\partial i_{dcr}}\Delta i_{dcr} \tag{25}$$

$$\Rightarrow \Delta P_{converter}=V_{dc0}\Delta i_{dcr}$$

$$s\left(C+C_p\right)\Delta V_{dc}=\frac{3}{2}\frac{v_{gq0}}{V_{dc0}}\Delta i_{gq}+\frac{3}{2}\frac{i_{gq0}}{V_{dc0}}\Delta v_{gq}-\frac{3}{2}\frac{v_{gq0}i_{gq0}}{V_{dc0}^2}\Delta V_{dc}+\frac{\Delta P_{converter}}{V_{dc0}} \tag{26a}$$

$$=\frac{3}{2}K_V\Delta i_{gq}+\frac{3}{2}K_G\Delta v_{gq}+\frac{1}{V_{dc0}}\Delta P_{converter}-\frac{3}{2}K_VK_G\Delta V_{dc}$$

From equation (26b), $K_V=\frac{v_{gq0}}{V_{dc0}}$ and $K_G=\frac{i_{gq0}}{V_{dc0}}$

Figs. 17 and 18 show the comparative analysis of the proposed DFIG supercapacitor scheme and the conventional DFIG parallel capacitor scheme. In Figs. 17 and 18, when the parallel capacitor was connected to the GSC of the DFIG power converter, better response was observed for the DC-link voltage and rotor speed of the wind generator, with fast recovery of the variables after transient state. The connection of the parallel converter at the RSC led to delayed recovery of the wind generator DC-link voltage and rotor speed variables. However, the proposed supercapacitor DFIG-based system for case 6 with optimal parameter ratings gave optimal changes than cases 3 and 4 and also the conventional DFIG parallel capacitor scheme.

B. Evaluation of the Proposed DFIG Supercapacitor System During Asymmetrical Faults at Super-synchronous and Sub-synchronous Speed

A further analysis of the performance of the proposed approach during super-synchronous as well as sub-synchronous speed was carried out in this section, as this will significantly affect the LVRT capability of the DFIG during asymmetrical faults. Figs. 19 to 24 show the responses of the DFIG wind turbine during super-synchronous speed, when the wind speed is above the nominal or rated wind speed and the sub-synchronous speed, when the wind speed is below the nominal or rated wind speed. In Figs. 19 and 20,-the performance of the DFIG DC-link voltage and terminal voltage were better during the super-synchronous speed than the sub-synchronous speed, during two line to ground fault scenario, because the wind generator is operating above its rated power during the fault scenario. Similarly, the same performance is expected for the line to line and line to ground faults in Figs. 21 to 24, for the DC-link voltage and terminal voltage of the DFIG wind turbine.

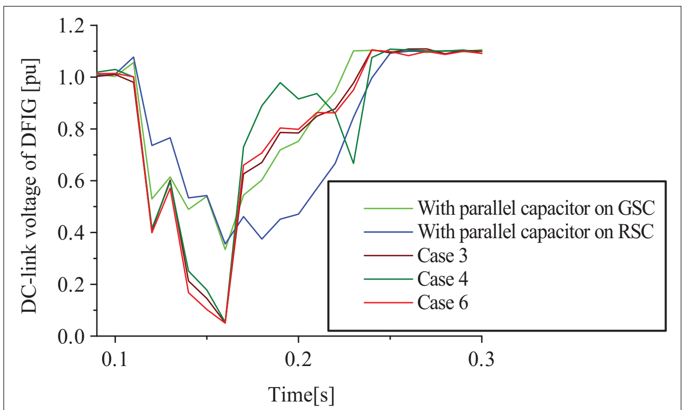

Fig. 17. DC-link voltage of doubly-fed induction generator wind turbine.

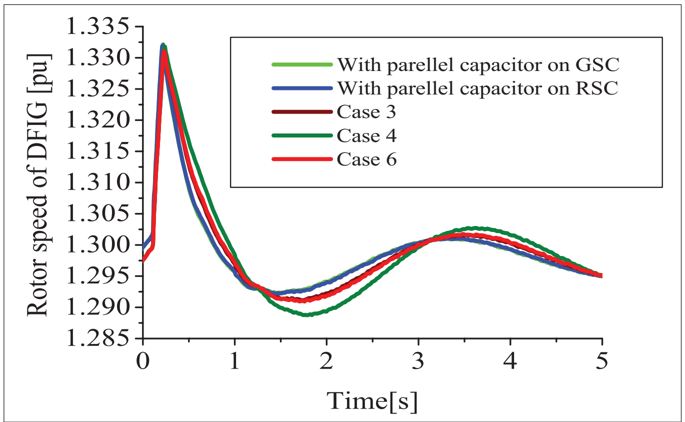

Fig. 18. Rotor speed of doubly-fed induction generator wind turbine.

C. Performance of the Proposed Scheme Under Zero-Voltage Condition at the Terminal of the Machine

In this section, the performance of the proposed scheme was evaluated under zero-voltage condition at the terminal of the DFIG wind turbine, as this issue has been demanded by most of the recent grid codes. In Fig. 25, the DC-link voltage of the wind generator reached almost zero during the transient state, and it was able to recover. Similarly, the terminal voltage of the DFIG wind turbine in Fig. 26 reached zero voltage and quickly recovered within the stipulated time set by the grid codes to remain connected to the grid after transient state. The impact of the zero voltage could also be seen in the response of the wind generator's rotor speed in Fig. 27. The rotor speed reaches a high oscillation value during the transient state and was able to regain stability within a short time to its steady state.

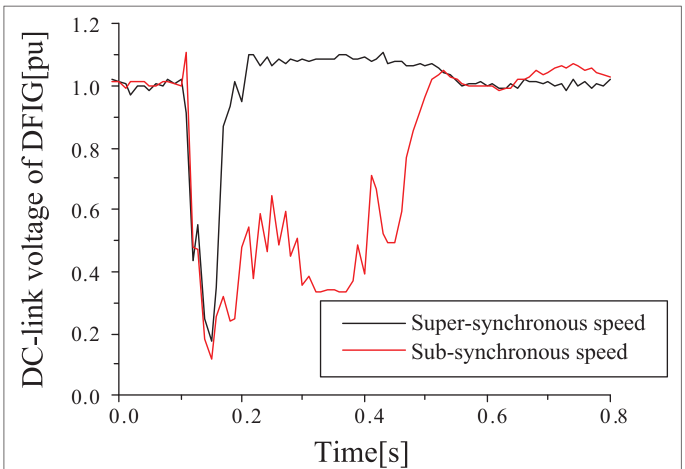

Fig. 19. DC-link voltage of doubly-fed induction generator wind turbine 2LG.

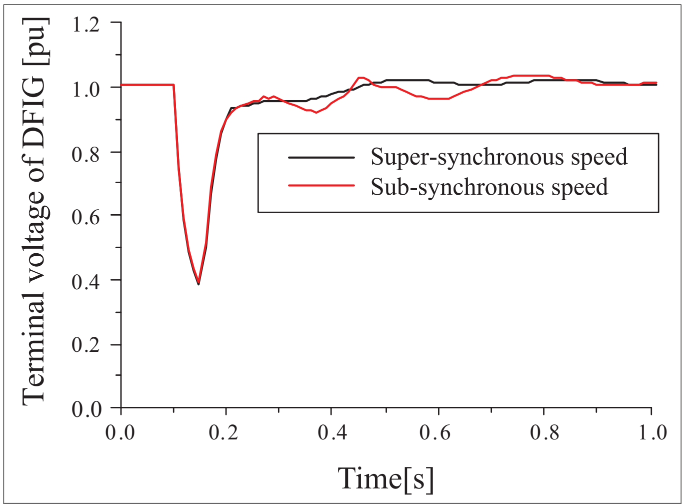

Fig. 20. Terminal voltage of doubly-fed induction generator wind turbine 2LG.

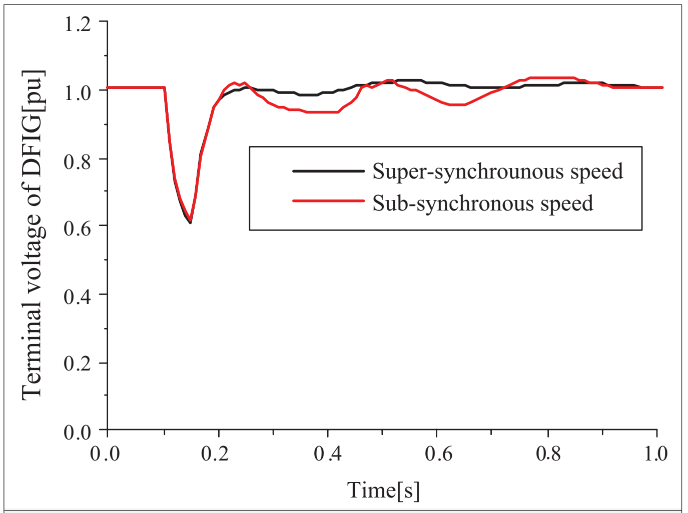

Fig. 22. Terminal voltage of doubly-fed induction generator wind turbine 2LL.

VII. CONCLUSION

The use of energy storage elements plays an important role in theoretically resolving transient problems in grid-connected DFIG-based wind turbines. This study investigated the effects of a supercapacitor, as an energy storage system, in DFIG transient stability. The supercapacitor was connected at the DC-link voltage, between the RSC and GSC of the DFIG wind turbine. The performance of the supercapacitor was investigated by varying its resistance, inductance, and capacitance parameters. A simple machine model system of DFIG and fixed-speed induction generator tied to an infinite bus was used in the study. The DC-link voltage and grid voltage were used for the switching of the supercapacitor. It was observed that when the resistance, capacitance, and inductance parameters of the supercapacitor were too small, the DC-link voltage and grid voltage switching strategies gave poor performances during transient state. However, the performance of the supercapacitor system in the DFIG was improved when the effective values of the parameters during transient state were used. The proposed supercapacitor DFIG scheme was compared to existing solutions in the literature,

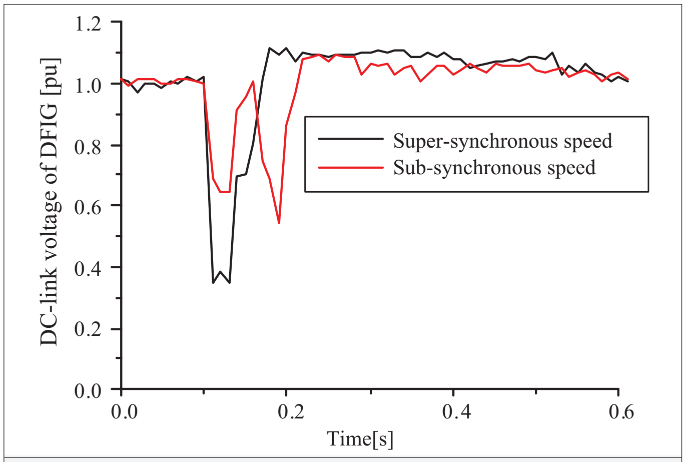

Fig. 23. DC-link voltage of doubly-fed induction generator wind turbine 1LG.

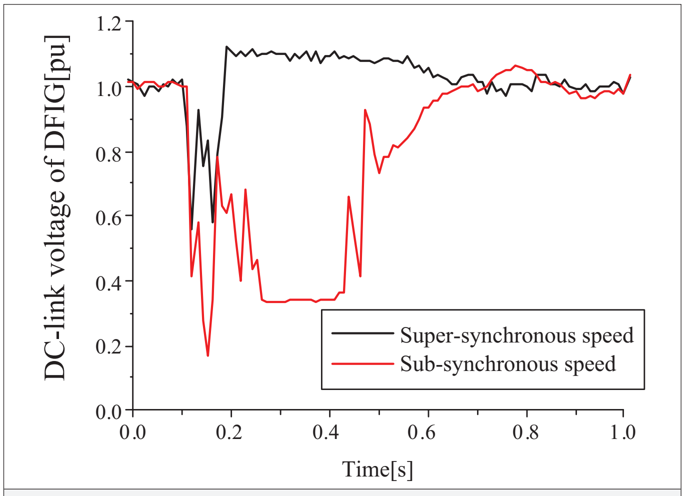

Fig. 21. DC-link voltage of doubly-fed induction generator wind turbine 2LL.

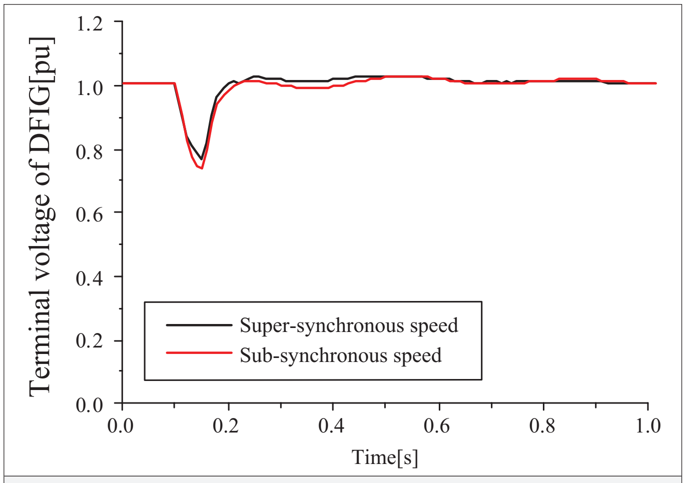

Fig. 24. DC-link voltage of doubly-fed induction generator wind turbine 1LG.

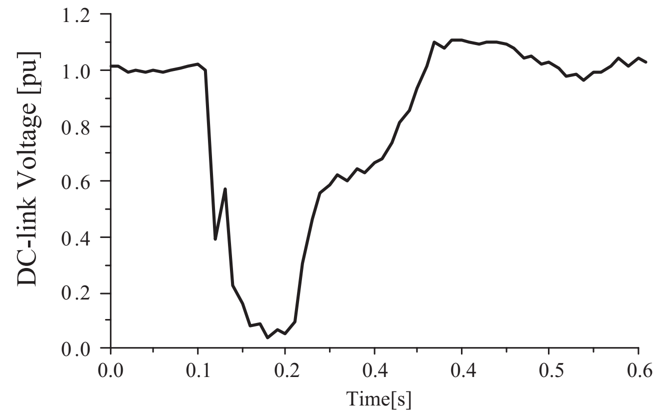

Fig. 25. DC-link voltage of doubly-fed induction generator wind turbine at zero voltage condition.

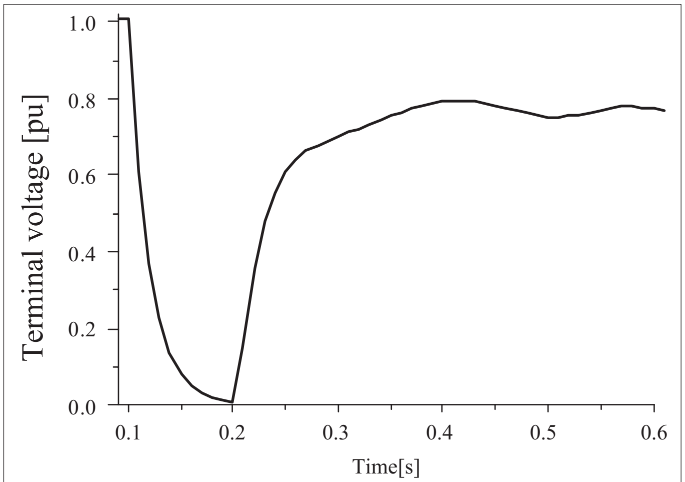

Fig. 26. Terminal voltage of doubly-fed induction generator wind turbine at zero voltage condition.

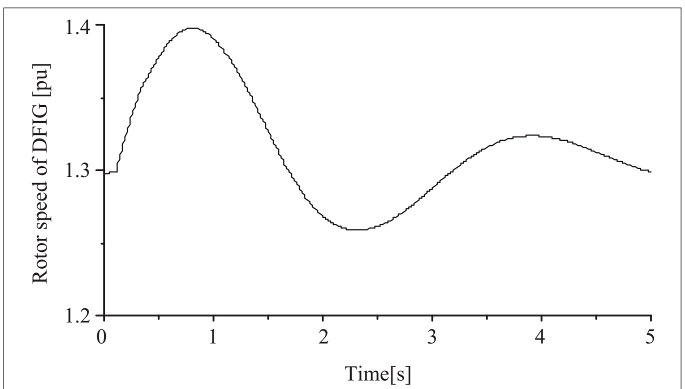

Fig. 27. Rotor speed of doubly-fed induction generator wind turbine at zero voltage condition.

using the parallel capacitor scheme for the DFIG, considering the same capacitance value. The obtained results show that the use of the existing parallel capacitor scheme in the DFIG GSC was able to enhance the performance of the DC-link voltage and rotor speed of the wind generator, with fast recovery of the variables after transient state, compared to when it is at the RSC of the DFIG. However, the proposed supercapacitor DFIG-based system with optimal parameter ratings gave optimal changes than the conventional DFIG parallel capacitor scheme.

Peer-review: Externally peer-reviewed.

Declaration of Interests: The author declare that they have no competing interest.

Funding: The author declared that this study has received no financial support.

REFERENCES

1. W. C. de Carvalho, R. P. Bataglioli, R. A. S. Fernandes, and D. V. Coury, "Fuzzy-based approach for power smoothing of a full-converter wind turbine generator using a supercapacitor energy storage," *Electr. Power Syst. Res.*, vol. 184, 2020. [CrossRef]
2. A. Hooshyar, M. A. Azzouz, and E. F. El-Saadany, "Three-phase fault direction identification for distribution systems with DFIG-based wind DG," *IEEE Trans. Sustain. Energy*, vol. 5, no. 3, pp. 747–756, 2014. [CrossRef]
3. M. M. Kabsha, and Z. H. Rather, "Advanced LVRT control scheme for offshore wind power plant," *IEEE Trans. Power Deliv.*, vol. 36, no. 6, 3893–3902, 2021. [CrossRef]
4. M. H. Zamani, G. Hossein Riahy, and M. Abedi, "Rotor-speed stability improvement of dual stator winding induction generator-based wind farms by control-windings voltage oriented control," *IEEE Trans. Power Electron.*, vol. 31, no. 8, pp. 5538–5546, 2016. [CrossRef].
5. R. Prasad, and N. P. Padhy, "Synergistic frequency regulation control mechanism for DFIG wind turbines with optimal pitch dynamics," *IEEE Trans. Power Syst.*, vol. 35, no. 4, pp. 3181–3191, 2020. [CrossRef]
6. A. M. A. Haidar, K. M. Muttaqi, and M. T. Hagh, "A coordinated control approach for DC link and Rotor Crowbars to improve fault ride-through of DFIG-based wind turbine," *IEEE Trans. Ind. Appl.*, vol. 53, no. 4, pp. 4073–4086, 2017. [CrossRef]
7. K. E. Okedu, S. M. Muyeen, R. Takahashi, and J. Tamura, "Wind farms fault ride through using DFIG with new protection scheme," *IEEE Trans. Sustain. Energy*, vol. 3, no. 2, pp. 242–254, 2012. [CrossRef]
8. D. Xie, Z. Xu, L. Yang, J. Østergaard, Y. Xue, and K. P. Wong, "A comprehensive LVRT control strategy for DFIG wind turbines with enhanced reactive power support," in *IEEE Trans. Power Syst.*, vol. 28, no. 3, pp. 3302–3310. [CrossRef]
9. J. Liang, W. Qiao, and R. G. Harley, "Feed-forward transient current control for low-voltage ride-through enhancement of DFIG wind turbines," *IEEE Trans. Energy Convers.*, vol. 25, no. 3, pp. 836–843. [CrossRef]
10. R. Hiremath, and T. Moger, "Comprehensive review on low voltage ride through capability of wind turbine generators, " *Int. Trans. Electr. Energy Syst.*, vol. 30, no. 10, 2020. [CrossRef]
11. Z. Zou, J. Liao, Y. Lei, Z. Mu, and X. Xiao, "Postfault LVRT performance enhancement of DFIG using a stage-controlled SSFCL-RSDR," *IEEE Trans. Appl. Supercond.*, vol. 29, no. 2, pp. 1–6. [CrossRef]
12. J. Vidal, G. Abad, J. Arza, and S. Aurtenechea, "Single-phase DC crowbar topologies for low voltage ride through fulfillment of high-power doubly Fed Induction Generator-Based Wind Turbines," *IEEE Trans. Energy Convers.*, vol. 28, no. 3, pp. 768–781. [CrossRef]
13. V. Yaramasu, B. Wu, S. Alepuz, and S. Kouro, "Predictive control for low-voltage ride-through enhancement of three-level-boost and NPC-converter-based PMSG wind turbine," *IEEE Trans. Ind. Electron.*, vol. 61, no. 12, pp. 6832–6843, Dec. 2014. [CrossRef]
14. O. P. Mahela, N. Gupta, M. Khosravy, and N. Patel, "Comprehensive overview of low voltage ride through methods of grid integrated wind generator," *IEEE Access*, vol. 7, pp. 99299–99326, 2019. [CrossRef]
15. S. Alepuz, A. Calle, S. Busquets-Monge, S. Kouro, and B. Wu, "Use of stored energy in PMSG rotor inertia for low-voltage ride-through in back-to-back NPC converter-based wind power systems," *IEEE Trans. Ind. Electron.*, vol. 60, no. 5, pp. 1787–1796, 2013. [CrossRef]
16. A. Calle-Prado, S. Alepuz, J. Bordonau, P. Cortes, and J. Rodriguez, "Predictive control of a back-to-back NPC converter-based wind power system," *IEEE Trans. Ind. Electron.*, vol. 63, no. 7, pp. 4615–4627, 2016. [CrossRef]

17. Z. Peng, and H. Yikang, "Control strategy of an active crowbar for DFIG based wind turbine under grid voltage dips," International Conference on Electrical Machines and Systems (ICEMS), Seoul, 2007, pp. 259–264.
18. L. Yang, Z. Xu, J. Ostergaard, Z. Y. Dong, and K. P. Wong, "Advanced control strategy of DFIG wind turbines for power system fault ride through," *IEEE Trans. Power Syst.*, vol. 27, no. 2, pp. 713–722. [CrossRef]
19. S. Xiao, G. Yang, H. Zhou, and H. Geng, "An LVRT control strategy based on flux linkage tracking for DFIG-based WECS," *IEEE Trans. Ind. Electron.*, vol. 60, no. 7, pp. 2820–2832. [CrossRef]
20. Q. Huang, X. Zou, D. Zhu, and Y. Kang, "Scaled current tracking control for doubly fed induction generator to ride-through serious grid faults," *IEEE Trans. Power Electron.*, vol. 31, no. 3, pp. 2150–2165, 2016. [CrossRef]
21. R. Zhu, Z. Chen, X. Wu, and F. Deng, "Virtual damping flux-based LVRT control for DFIG-based wind turbine," *IEEE Trans. Energy Convers.*, vol. 30, no. 2, pp. 714–725, 2015. [CrossRef]
22. D. Zhu, X. Zou, S. Zhou, W. Dong, Y. Kang, and J. Hu, "Feedforward current references control for DFIG-based wind turbine to improve transient control performance during grid faults," *IEEE Trans. Energy Convers.*, vol. 33, no. 2, pp. 670–681, 2018. [CrossRef]
23. J. Bhukya, and V. Mahajan, "Optimization of damping controller for PSS and SSSC to improve stability of interconnected system with DFIG based wind farm," *Int. J. Electr. Power Energy Syst.*, vol. 108, pp. 314–335, 2019. [CrossRef]
24. M. J. Hossain, T. K. Saha, N. Mithulananthan, and H. R. Pota, "Control strategies for augmenting LVRT capability of DFIGs in interconnected power systems," *IEEE Trans. Ind. Electron.*, vol. 60, no. 6, pp. 2510–2522, 2013. [CrossRef]
25. M. J. Hossain, H. R. Pota, V. A. Ugrinovskii, and R. A. Ramos, "Simultaneous STATCOM and pitch angle control for improved LVRT capability of fixed-speed wind turbines," *IEEE Trans. Sustain. Energy*, vol. 1, no. 3, pp. 142–151, 2010. [CrossRef]
26. I. M. Syed, B. Venkatesh, B. Wu, and A. B. Nassif, "Two-layer control scheme for a supercapacitor energy storage system coupled to a doubly fed induction generator," *Electr. Power Syst. Res.*, vol. 86, pp. 76–83, 2012. [CrossRef]
27. L. Qu, and W. Qiao, "Constant power control of DFIG wind turbines with supercapacitor energy storage," *IEEE Trans. Ind. Appl.*, vol. 47, no. 1, pp. 359–367, 2011. [CrossRef]
28. V. Krishnamurthy, and C. R. Kumar, "A novel two layer constant power control of 15 DFIG wind turbines with supercapacitor energy storage," *Int. J. Adv. Innov.*, vol. 2, pp. 68–77, 2013.
29. S. Dongyang, Z. Xiongxin, S. Lizhi, W. Fengjian, and Z. Guangxin, "Study on power fluctuation suppression of DFIG based on super capacitor energy storage," In *2017 IEEE Conference on Energy Internet and Energy System Integration (EI2)*, Beijing, China: IEEE Publications, 2017, pp. 1–6.
30. R. Suryana, "Frequency control of standalone wind turbine with supercapacitor," In *33rd International Telecommun. Energy Conference (INTELEC)*, Amsterdam, Netherlands: IEEE Publications, 2011, pp. 1–8.
31. R. Aghatehrani, R. Kavasseri, and R. C. Thapa, "Power smoothing of the DFIG wind turbine using a small energy storage device," In *IEEE PES Gen Meeting*. Minnesota, USA: IEEE Publications, 2010, pp. 1–6.
32. N. Mendis, K. M. Muttaqi, and S. Perera, Active Power Management of a Supercapacitor-Battery Hybrid Energy Storage System for Standalone Operation of DFIG Based Wind Turbines. *IEEE Industry Applications Society Annual Meeting*. Las Vegas, USA, 7–11 October, 2012.
33. E. Naswali *et al.*, Supercapacitor Energy Storage for Wind Energy Integration. *IEEE Energy Conversion Congress and Exposition*, Phoenix, Arizona, 17–22 September, 2011.
34. S. Huang, Q. Wu, Y. Guo, and F. Rong, "Optimal active power control based on MPC for DFIG-based wind farm equipped with distributed energy storage systems," *Int. J. Electr. Power Energy Syst.*, vol. 113, pp. 154–163, 2019. [CrossRef]
35. T. Wei, S. Wang, and Z. Qi, "Design of supercapacitor based ride through system for wind turbine pitch systems," In International Conference on Electrical Machines and Systems (ICEMS), IEEE Publications, 2007, pp. 294–297.
36. S. M. Muyeen, R. Takahashi, M. H. Ali, T. Murata, and J. Tamura, "Transient stability augmentation of power system including wind farms by using ECS," *IEEE Trans. Power Syst.*, vol. 23, no. 3, pp. 1179–1187, 2008. [CrossRef]
37. N. Mendis, K. M. Muttaqi, S. Sayeef, and S. Perera, "Application of a hybrid energy storage in a remote area power supply system," *IEEE International Energy Conference*, IEEE Publications, 2010, pp. 576–581.
38. X. Li, C. Hu, C. Liu, and D. Xu, "Modeling and control of aggregated supercapacitor energy storage system for wind power generation," In 34th Annual Conference of IEEE Industrial Electronics, IEEE Publications, 2008, pp. 3370–3375.
39. H. Babazadeh, W. Gao, and X. Wang, "Controller design for a hybrid energy storage system enabling longer battery life in wind turbine generators," In North American Power Symposium, Boston, MA, USA: IEEE Publications, 4-6 Aug. 2011. DOI: 10.1109/NAPS.2011.6025178.
40. M. F. M. Arani, and E. F. El-Saadany, "Implementing virtual inertia in DFIG-based wind power generation," *IEEE Trans. Power Syst.*, vol. 28, no. 2, pp. 1373–1384, 2013. [CrossRef]
41. D. Yang, H. C. Gao, L. Zhang, T. Zheng, L. Hua, and X. Zhang, "Short-term frequency support of a doubly-fed induction generator based on an adaptive power reference function," *Int. J. Electr. Power Energy Syst.*, vol. 119, 2020. [CrossRef]
42. J. Zhu *et al.*, "Synthetic inertia control strategy for doubly fed induction generator wind turbine generators using lithium-ion supercapacitors," *IEEE Trans. Energy Convers.*, vol. 33, no. 2, pp. 773–783, 2017. [CrossRef]
43. L. Xiong, Y. Li, Y. Zhu, P. Yang, and Z. Xu, "Coordinated control schemes of super-capacitor and kinetic energy of DFIG for system frequency support," *Energies*, vol. 11, no. 1, p. 103, 2018. [CrossRef]
44. S. S. Sahoo, K. Chatterjee, and P. M. Tripathi, "A coordinated control strategy using supercapacitor energy storage and series dynamic resistor for enhancement of fault ride-through of doubly fed induction generator," *Int. J. Green Energy*, vol. 16, no. 8, pp. 615–626, 2019. [CrossRef]
45. O. Noureldeen, and M. M. Youssef, "Super-capacitor utilization for low voltage ride through improvement of grid-tied wind turbines," In Nineteenth International Middle East. Power Syst. Conference (MEPCON), IEEE Publications, 2017, pp. 1305–1309.
46. M. Garcia-Garcia, M. P. Comech, J. Sallan, and A. Liombart, "Modelling Wind Farms for Grid Disturbances Studies," *Science Direct Renew. Energy*, vol. 33, pp. 2019–2026, 2008.
47. K. E. Okedu, S. M. Muyeen, R. Takahashi, and J. Tamura, "Application of SDBR with DFIG to Augment Wind Farm Fault Ride Through," 24th IEEE-ICEMS (International Conference on Electrical Machines and Systems), Beijing, China, 2011, pp. 1–6.
48. K. E. Okedu, "Enhancing the performance of DFIG variable speed wind turbine using parallel integrated capacitor and modified modulated braking resistor," *IET Gener. Transm. Distrib.*, vol. 13, no. 15, pp. 3378–3387, 2019. [CrossRef]
49. K. E. Okedu, "Improving the transient performance of DFIG wind turbine using pitch angle controller low pass filter timing and network side connected damper circuitry," *IET Renew. Power Gener.*, vol. 14, no. 7, pp. 1219–1227, 2020. [CrossRef]
50. I. Zubia, J. X. Ostolaza, A. Susperrgui, and J. J. Ugartemendia, "Multi-machine transient modeling of wind farms, an essential approach to the study of fault conditions in the distribution network," *Appl. Energy*, vol. 89, no. 1, pp. 421–429, 2012. [CrossRef]
51. X. Kong, Z. Z. Xianggen, and M. Wen, "Study of fault current characteristics of the DFIG considering dynamic response of the RSC," *IEEE Trans. Energy Convers.*, vol. 2, no. 2, pp. 278–287, 2014.
52. A. B. Cultura, and Z. M. Salameh, "Modeling, evaluation and simulation of a supercapacitor module for energy storage application," In International Conference on Computer Information Systems and Industrial Applications, Atlantis Press, 2015.
53. M. K. Döşoğlu, and A. B. Arsoy, "Transient modeling and analysis of a DFIG based wind farm with supercapacitor energy storage," *Int. J. Electr. Power Energy Syst.*, vol. 78, pp. 414–421, 2016. [CrossRef]
54. M. K. Döşoğlu, "Nonlinear dynamic modeling for fault ride-through capability of DFIG-based wind farm," *Nonlinear Dyn.*, vol. 89, no. 4, pp. 2683–2694, 2017. [CrossRef]
55. R. Isermann, and M. Münchhof, *Identification of Dynamic Systems: An Introduction with Applications*. Berlin, Germany: Springer Science & Business Media, 2010.
56. Y. Wang, C. Liu, R. Pan, and Z. Chen, "Modeling and state-of-charge prediction of lithium-ion battery and ultracapacitor hybrids with a co-estimator," *Energy*, vol. 121, pp. 739–750, 2017. [CrossRef]
57. M. Ceraolo, G. Lutzemberger, and D. Poli, "State-of-charge evaluation of supercapacitors," *J. Energy Storage*, vol. 11, pp. 211–218, 2017. [CrossRef]
58. M. Henry, B. Andrés, F. Cristina, Z. Pablo, L. Antonio, and A. General, "Parameter identification procedure used for the comparative study of supercapacitors models," *Energies*, vol. 12, no. 1776, pp. 1–20, 2019.
59. "PSCAD/EMTDC manual," *Manit. HVDC Lab*, 2016.

Kenneth Eloghene Okedu was a research fellow in the Department of Electrical and Computer Engineering, Massachusetts Institute of Technology (MIT), Boston, USA, in 2013. He obtained his PhD from the Department of Electrical and Electronic Engineering, Kitami Institute of Technology, Japan, in 2012. He received his BSc and MEng in Electrical and Electronic Engineering from the University of Port Harcourt, Nigeria, in 2003 and 2007, respectively, where he was retained as a faculty member from 2005 until the present day. He has also been a visiting faculty member at the Abu Dhabi National Oil Company (ADNOC) Petroleum Institute. He was also a visiting faculty member at the Caledonian College of Engineering, Oman (Glasgow Caledonian University, UK). He is presently a visiting professor in the Department of Electrical and Computer Engineering, National University of Science and Technology (NUST), Oman, and an adjunct professor in the Department of Electrical and Electronic Engineering, Nisantasi University, Turkey. He was recognized as a top 1% peer reviewer in Engineering by Publons in 2018 and 2019 and was the editor's pick in the *Journal of Renewable and Sustainable Energy* in 2018. Dr. Okedu has published several books and journals/transactions in the field of renewable energy. He is an editorial board member for journals including *Frontiers in Renewable Energy Research in Smart Grids*, *International Journal of Electrical Engineering*, *Mathematical Problems in Engineering*, and *Trends in Renewable Energy*. His research interests include power system stability, renewable energy systems, stabilization of wind farms, stability analysis of doubly-fed induction generators and permanent magnet synchronous generators variable speed wind turbines, augmentation and integration of renewable energy into power systems, grid frequency dynamics, wind energy penetration, FACTS devices and power electronics, renewable energy storage systems, and hydrogen and fuel cells.